PCCP

Accepted Manuscript

ROYAL SOCIETY OF CHEMISTRY

www.rsc.org/pccp

Cite this: DOI: 10.1039/c0xx00000x

www.rsc.org/xxxxxx

Communication

Spontaneous Dimer States of the Aβ$_{21-30}$ Decapeptide

Micholas Dean Smith[a], J. Srinivasa Rao[b] and Luis Cruz*[a]

Received (in XXX, XXX) Xth XXXXXXXXX 200X, Accepted Xth XXXXXXXXX 200X

First published on the web Xth XXXXXXXXX 200X

DOI: 10.1039/b00000000x

Constant temperature and replica-exchange molecular dynamics simulations of two Aβ$_{21-30}$ decapeptides in explicit solvent reveal metastable dimers states that are abundant near physiological temperatures. As Alzheimer's disease is associated with the neurotoxic oligomers of amyloid β-protein, the formation of these dimers provide insight into oligomer assembly.

In recent years, low-weight oligomeric species of the amyloid β-protein (Aβ) have been shown to be the proximal neurotoxic agents associated with Alzheimer's disease (AD)[1-10]. As a result of this, a number of studies using experimental[7,11-18] and computational[19-30] methods have focused on the early stages of Aβ oligomerization, ranging from monomer (mis)folding to early stage (dimers, tetramers, pentamers, and other) oligomer structures. Particularly interesting findings from these studies include: the structure of these oligomers are different from previously characterized amyloid fibrils[15], two different aggregation pathways may exist for Aβ with one leading to oligomers and another to fibrils[18], a turn/bend exists in the 20-30 region[19,29], and both parallel and anti-parallel β-sheets exist for fibril and oligomer aggregates of Aβ$_{1-40/42}$ oligomers[15] (though the parallel state is rare for oligomers[18,19]).

Interestingly, the 21-30 region not only contributes a common structural motif between oligomeric forms of Aβ, but has inter-peptide salt-bridges between Lys28 and Glu22/Asp23 residues which may act as a limiting step in oligomer aggregation and/or fibril generation[25,30]. Mutations in this region have also been shown to modify the structure of Aβ aggregates (fibrils and oligomers)[16,20,31,32] as well as their neurotoxicity[7,16].

In addition to its role in Aβ oligomers, Lazo et al suggested that the 21-30 region, as well as the 21-30 decapeptide fragment, are protease resistant, indicating that this region is the folding nucleus for the monomeric form of Aβ[33]. A number of investigations by Cruz et al[34,35] and others[33,36-42] have further characterized this fragment as an intrinsically disordered protein (IDP); exhibiting coil, turn, and meta-stable extended β-hairpin secondary structure motifs with the latter structure supported by intra-peptide hydrogen-bonding and salt-bridge formation between Lys28 and Glu22/Asp23 residues.

As this region is an IDP, is likely the folding nucleus of monomeric full-length Aβ[33], presents common motifs for a variety of aggregate structures[33,42], and its behavior is associated with possible rate limiting steps[25,30] (structural rearrangement and or inter-peptide salt-bridging) in the oligomerization and/or fibrillation process, investigation of the potential dimerization of isolated fragments of the 21-30 region (Aβ$_{21-30}$) is of importance. Further, we hypothesize that short-lived dimer states for this isolated decapeptide may exist and be driven by non-hydrophobic interactions and that demonstration of these states may provide insight into the earliest stages of association in the full-length peptide.

Here we use constant temperature all-atom molecular dynamics simulations (MD) with explicit solvent to study both the spontaneous formation of Aβ$_{21-30}$ decapeptide dimers and their mean exit time (i.e. lifetimes) from specific dimer conformations. Additionally, we use replica exchange molecular dynamics (REMD) simulations to study the temperature dependent stability of these dimers.

The Aβ$_{21-30}$ studied here has the amino acid sequence AEDVGSNKGA with uncapped and oppositely charged ends. All simulations used the OPLS/AA force field[43,44] with TIP3P[45] water, and were carried out with the GROMACS software package[46-49]. The choice of OPLS/AA was mainly guided by its lack of uncharacteristic helices in this particular peptide, and as an alternative to using newer versions of AMBER and CHARMM which have otherwise been shown to perform well for other "amyloid peptides." [50,51] To neutralize the system, two Na^+ ions were added to the system. As constructed, the system had neutral pH. To study the dynamics of dimer formation and determine dimer lifetimes we used constant temperature (serial) NPT simulations at a temperature of 283K (to correspond with previous work[33-35]) and a pressure of 1 atm, being held constant by the Berendsen baro/thermostats[46] and with a timestep of 4 fs. To simulate dimer formation, we generated twenty independent, 400 ns long trajectories with the initial condition of two parallel monomer chains of Aβ$_{21-30}$ spatially separated (by a minimum distance of 15Å) in random-coil (open) secondary structure configurations. It should be noted that by using the initial condition of two parallel separated monomers, a bias in the type of dimers produced will occur; however, the goal of the serial simulations was simply to identify and characterize any naturally (dynamically) occurring dimers regardless of the relative abundances of dimer types. Dimer lifetimes were investigated by generating twenty, 350 ns long trajectories,

with half of the simulations having an initial configuration of an anti-parallel dimer, while the other half having a parallel dimer configuration.

For the REMD simulations, two trajectories, one with the initial condition of a parallel dimer configuration and the other with an anti-parallel configuration, of length 150 ns/replica and timestep of 2 fs were generated. The REMD simulations used 48 temperatures in the range from 276 to 405K, and was chosen to both focus on experimentally relevant temperatures and obtain an average exchange rate of ~30%[52]. The REMD trajectories were generated using the Nose-Hoover[53] thermostat, Parrinello-Rahman[54,55] barostat. Explanations concerning the simulation details and convergence are provided in the supporting information (Table S1 and Figure S1).

To characterize the equilibrium ensemble we used as order parameters: (i) the dot product of each chain's end-to-end vector (P_e) and (ii) the number of inter-peptide hydrogen-bonds (HB - taken with cut-offs of 3Å and 20°). Based on these order parameters, three regions of interest in conformational space were defined, where the first two, regions I and II, contained structures with a number of inter-peptide HBs greater than or equal to 3, and chain end-to-end vector dot products less than or equal to -0.7 for region I and greater than or equal to 0.7 for region II (see typical conformations in Figure 1). The choice of 3 or more HBs as a characterizing factor was chosen as the more rigorous and strict cutoff for dimer identification that would lessen the number of tail-to-tail, head-to-head, and tail(head)-to-head(tail) states while identifying more compact parallel and anti-parallel states.

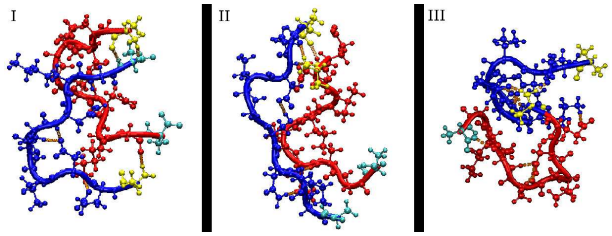

Figure 1. Typical conformations from each defined structure: I (anti-parallel), II (parallel), and III (unaligned dimers).

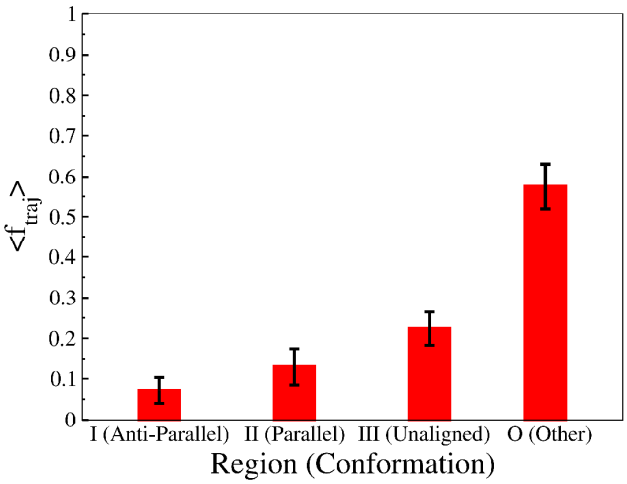

Figure 2. Average fraction of conformations belonging to each conformational family from the constant temperature trajectories. Error bars are the standard error of the mean.

Other dimer states with inter-peptide HBs greater than 2 but with a value of P_e not corresponding with Regions I or II were noted as region III, and labeled "unaligned dimers." All other states were assigned to Region O, defined to contain all structures with 2 or fewer inter-peptide HBs (consisting of free monomers and highly-disordered aggregates), which we labeled "other." Figure 2 shows the average fraction of conformations belonging to each region calculated using the serial simulations starting from parallel separated monomers. From this figure, it is clear that the peptides reside in one of the three dimeric conformation (either region I, II, or III) for approximately half of the total simulation time. It should be noted that because the initial configurations of the simulations contained the separated monomers in a parallel alignment, a bias may be present for the formation of parallel dimers, but the existence of both parallel and anti-parallel demonstrate that both dimer states can spontaneously form.

When doing a histogram of conformations in our parameter space to produce an energy landscape (inter-peptide HBs and P_e) shown in Figure 3, we find that the anti-parallel and parallel structures are independently located at local minimums of the energy. Additionally, the region of the energy landscape associated with the III dimer states is nearly flat with a very small minima indicating that these III unaligned dimer states are widely varied in structure and that they can easily transition between themselves.

Computation of inter-peptide HB contact maps, Figure 4, shows that the anti-parallel state is composed largely of inter-peptide Ala21-Ala30, Glu22-Lys28, and Asn27-Asn27 contacts; while parallel states are made up of Glu22-Glu22 and Asp23-Asp23 contacts. An interesting note is that the Glu22-Lys28 contacts from the anti-parallel states have been characterized in other contexts, such as in forming the meta-stable β-hairpin associated with the monomer form of the peptide[34,35,56-58].

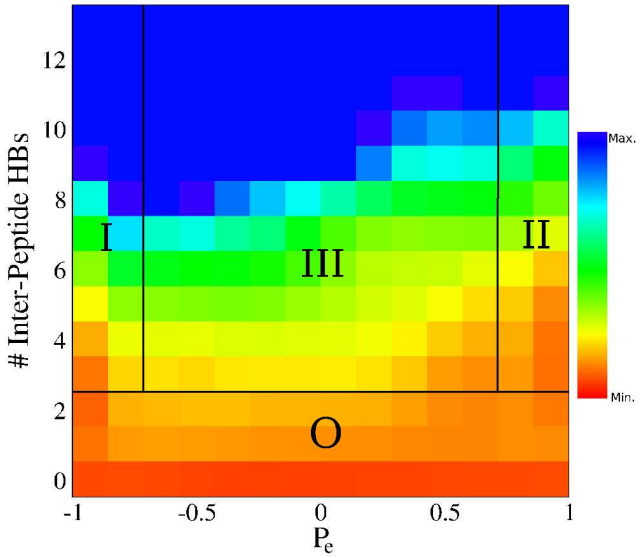

Figure 3. Relative Free-energy landscape constructed by using values of the Chain End-to-End dot-products (P_e) and inter-peptide HBs from constant temperature trajectories. Roman numerals correspond to conformations in Figure 1.

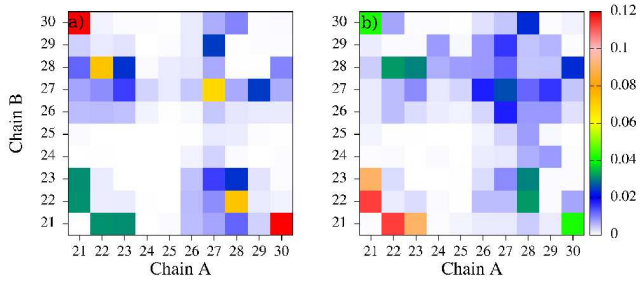

Figure 4. Inter-peptide HB contact maps for: a) anti-parallel, and b) parallel dimers. Different colours correspond to the fraction of the total number of inter-peptide HBs for that corresponding dimer.

Results from the analysis of the secondary structure per amino acid from these same serial trajectories, using STRIDE[59,60] are shown in Figure 5. These data show that on average the secondary structures of each monomer are similar to each other with dominating turn and coil structures, and minor peaks in the β-bridge and extended β-sheet conformations. There are, however, some key differences, such as the anti-parallel (region I) state having reduced C-termini coil propensities and higher propensities for extended conformations throughout the peptide, while the parallel state has substantially higher bridging propensities (see Figure S2 in the SI).

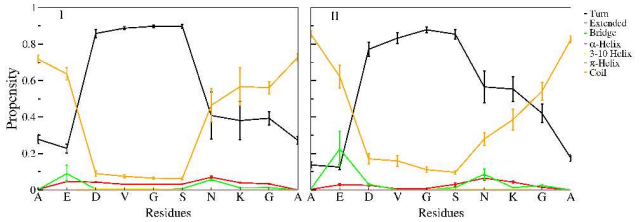

Figure 5. Average per-residue secondary structure propensities for dimers of type I and II. Error bars are weight adjusted variances.

An important observation is that on comparing the secondary structure propensities of the anti-parallel dimer states with those of isolated monomers (from Cruz et al[34] and others[38,42]), the secondary structure and register of HBs are similar to the intra-peptide register of the meta-stable β-hairpin structure, suggesting that the structure found in the monomeric β-hairpin structures is preserved in these dimer-states.

Having determined the existence and structure of the dimers, we now turn to investigate the stability of each of these dimer states. For this, we performed two separate measurements. In the first, the lifetimes of the dimer states at a temperature of 283K were computed (see SI for details), with longer lifetimes corresponding to higher degrees of stability. In the second method, the relative populations of anti-parallel and parallel dimer states from the last 100ns of two independent REMD simulations (one with an initial anti-parallel dimer conformation and the other with an initial parallel dimer conformation) were calculated. One point of caution is that while these measurements provide information regarding the stability of regions I and II relative to the energy barrier between the dimer conformations, they do not necessarily contain information regarding dimer dissociation or association rates.

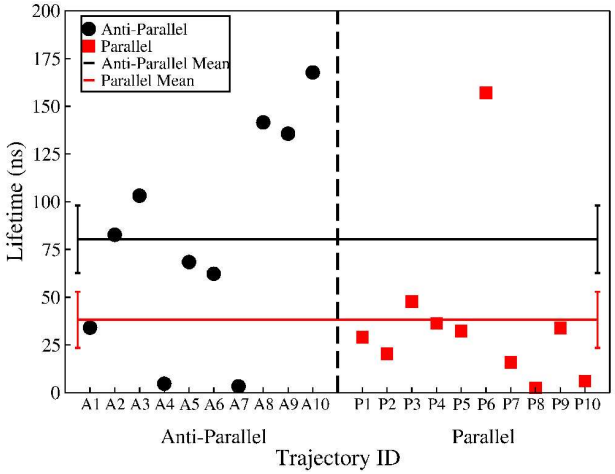

Figure 6. Dimer lifetimes for each trajectory. Averages are represented as horizontal lines with error bars representing the standard error of the mean.

Using data from the REMD simulations, we generated both relative energy maps (Figure 7) and measures of population fractions (Figure 8). These data suggest that both dimeric conformations are abundant at temperatures at or below 330K, and of these the anti-parallel may be more prevalent (see Figure S3 in the SI for additional temperatures).

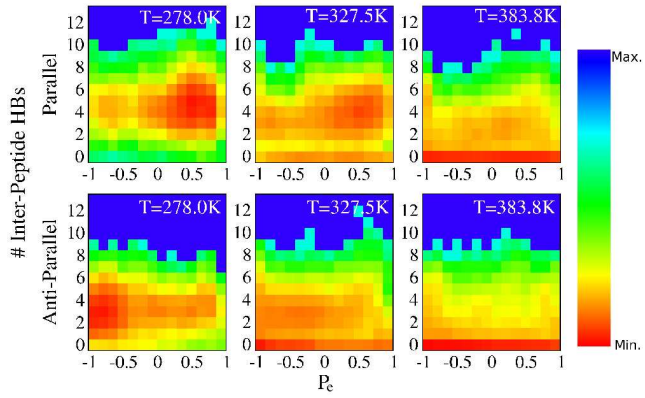

Figure 7. Relative Free-energy landscapes at different temperatures for the last 100 ns of both parallel (top row) and anti-parallel dimer conformations from the REMD simulations. Normalization is preserved across temperatures and dimer types allowing for direct comparison. Red/Blue indicate minima and maxima, respectively.

To quantify which of the two dimers is more stable over the tested temperature range, the fraction of conformations of a given dimer type per replica temperature (Figure 8) was calculated. These data reveal that at or below physiological temperatures (310 K), anti-parallel dimers (region I) are more prevalent (and thus more stable) than parallel dimers (region II).

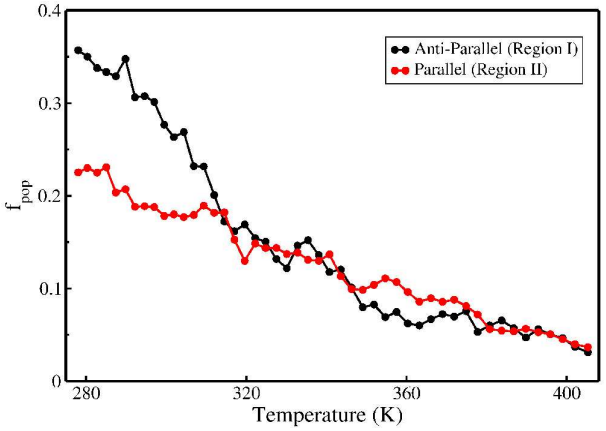

Figure 8. Population fractions of the I and II region dimer conformations as a function of temperature. The fractions are measured using the last 100 ns from each REMD trajectory. A similar figure that includes monomer populations is presented in Figure S4 of the SI.

In sum, using serial MD simulations we have shown that the $A\beta_{21-30}$ decapeptide fragment may spontaneously dimerize into both anti-

parallel and parallel conformations. Furthermore, these serial simulations revealed that the anti-parallel and parallel states have only minor differences between their secondary structures, and that the anti-parallel state has inter-peptide HBs with similar registers as intra-peptide HBs found in the meta-stable β -hairpin motif of the isolated monomers, which is in close correspondence to work by Anand et al[25]. These two facts indicate the strong influence that the structure of the monomer has on the structure of the dimer.

In addition, by using REMD and serial lifetime simulations, we were able to determine that of the two dimer configurations, the anti-parallel appears more frequently than the parallel state at physiological temperatures and has a greater lifetime at 283K, suggesting that it is likely more stable than the parallel one. The observation that average lifetimes of these states are in the sub-microsecond regime plus the observation (from the REMD) that populations of the dimers near physiological temperatures are found to be at most ~25% suggest that both dimeric states are meta-stable. Furthermore, our observation that anti-parallel states are more stable than parallel states suggests that low weight oligomers may gain some degree of stability by forming anti-parallel motifs, corresponding to the observation by Cerif et al[18] that oligomeric forms of Aβ are significantly anti-parallel in make up.

It is interesting that the spontaneous dimer states reported here had previously not been observed in experimental work of Lazo et al[33] and Fawi et al[39]. Our observations of such short lifetimes and overall meta-stability of these states, along with differences in solvent conditions, suggest that dimer state signals (if any) from these experiments would be relatively weak, that without an *a priori* knowledge that dimer states would likely passed unnoticed. Additionally, the differences between our simulations, an estimated concentration of ~22mM (nearly double that of Lazo et al[33]) and lack of ammonium (as used by Fawzi et al[39]), may also account for the discrepancies with experiment. It is the hope of this work that by highlighting the characteristics of these dimer states, existing experimental results might be re-evaluated or new experiments could be performed to validate the spontaneous dimer states reported here.

Acknowledgements: Computational time was partially provided by XSEDE computational resources grant TG-MCB110142.

Notes and references

*Corresponding Author: Luis Cruz
[a] 3141 Chestnut Street, Drexel University, Department of Physics, Philadelphia, USA
E-mail: ccruz@drexel.edu
[b] New Jersey Institute of Technology, Department of Physics, University Heights, Newark, NJ, USA

† Electronic Supplementary Information (ESI) available: Further simulation details and additional REMD generated energy landscapes. See DOI: 10.1039/b000000x/

1 Hardy J & Selkoe DJ, *Science*, 2002, **297**, pp. 353-356.
2 Kirkitadze MD, Bitan G & Teplow DB, *J. Neurosci. Res.*, 2002, **69**, pp. 567-577.
3 Klein WL, Stine WBJ & Teplow DB, *Neurobiol. Aging*, 2004, **25**, pp. 569-580.
4 Lambert MP, Barlow AK, Chromy BA, Edwards C, Freed R, Liosatos M, Morgan TE, Rozovsky I, Trommer B, Viola KL, Wals P, Zhang C, Finch CE, Krafft GA & Klein WL, *Proc. Natl. Acad. Sci. U.S.A.*, 1998, **95**, pp. 6448-6453.
5 Lesne S, Koh M, Kotilinek L, Kayed R, Glabe C, Yang A, Gallagher M & Ashe K, *Nature*, 2006, **440**, pp. 352-357.
6 Ono K & Yamada M, *J. Neurochem.*, 2011, **117**, pp. 19-28.
7 Ono K, Condron MM & Teplow DB, *Proc. Natl. Acad. Sci. U.S.A.*, 2009, **106**, pp. 14745-14750.
8 Roychaudhuri R, Yang M, Hoshi MM & Teplow DB, *J. Biol. Chem.*, 2009, **284**, pp. 4749-4753.
9 Walsh DM, Klyubin I, Shankar GM, Townsend M, Fadeeva JV, Betts V, Podlisny MB, Cleary JP, Ashe KH, Rowan MJ & Selkoe DJ, *Biochem. Soc. Trans.*, 2005, **33**, pp. 1087-1090.
10 Walsh DM & Selkoe DJ, *J. Neurochem.*, 2007, **101**, pp. 1172-1184.
11 Bitan G, Lomakin A & Teplow DB, *J. Biol. Chem.*, 2001, **276**, pp. 35176-35184.
12 Hou L, Shao H, Zhang Y, Li H, Menon NK, Neuhaus EB, Brewer JM, Byeon IL, Ray DG, Vitek MP, Iwashita T, Makula RA, Przybyla AB & Zagorski MG, *J. Am. Chem. Soc.*, 2004, **126**, pp. 1992-2005.
13 Bitan G, Vollers SS & Teplow DB, *J. Biol. Chem.*, 2003, **278**, pp. 34882-34889.
14 Soreghan B, Kosmoski J & Glabe C, *J. Biol. Chem.*, 1994, **269**, pp. 28551-28554.
15 Yu L, Edalji R, Harlan JE, Holzman TF, Lopez AP, Labkovsky B, Hillen H, Barghorn S, Ebert U, Richardson PL, Miesbauer L, Solomon L, Bartley D, Walter K, Johnson RW, Hajduk PJ & Olejniczak ET, *Biochemistry*, 2009, **48**, pp. 1870-1877.
16 Peralvarez-Marin A, Mateos L, Zhang C, Singh S, Cedazo-Minguez A, Visa N, Morozova-Roche L, Graslund A & Barth A, *Biophys. J*, 2009, **97**, pp. 277-285.
17 Sciarretta KL, Gordon DJ, Petkova AT, Tycko R & Meredith SC, *Biochemistry*, 2005, **44**, pp. 6003-6014.
18 Cerf E, Sarroukh R, Tamamizu-Kato S, Breydo L, Derclaye S, Dufrêne YF, Narayanaswami V, Goormaghtigh E, Ruysschaert J & Raussens V, *Biochem. J.*, 2009, **421**, pp. 415-423.
19 Mitternacht S, Staneva I, Härd T & Irbäck A, *J. Mol. Biol.*, 2011, **410**, pp. 357-367.
20 Côté S, Laghaei R, Derreumaux P & Mousseau N, *J Phys Chem B*, 2012, **116**, pp. 4043-4055.
21 Barz B & Urbanc B, *PLoS ONE*, 2012, **7**, p. e34345.
22 Zhu X, Bora RP, Barman A, Singh R & Prabhakar R, *J Phys Chem B*, 2012, **116**, pp. 4405-4416.
23 Zhao J, Wang Q, Liang G & Zheng J, *Langmuir*, 2011, **27**, pp. 14876-14887.
24 Tarus B, Straub JE & Thirumalai D, *J. Mol. Biol.*, 2005, **345**, pp. 1141-1156.
25 Anand P, Nandel FS & Hansmann UHE, *J Chem Phys*, 2008, **129**, p. 195102.
26 Chebaro Y, Mousseau N & Derreumaux P, *J Phys Chem B*, 2009, **113**, pp. 7668-7675.
27 Urbanc B, Cruz L, Teplow DB & Stanley HE, *Curr Alzheimer Res*, 2006, **3**, pp. 493-504.
28 Urbanc B, Cruz L, Yun S, Buldyrev SV, Bitan G, Teplow DB & Stanley HE, *Proc. Natl. Acad. Sci. U.S.A.*, 2004, **101**, pp. 17345-17350.
29 Petkova AT, Ishii Y, Balbach JJ, Antzutkin ON, Leapman RD, Delaglio F & Tycko R, *Proc. Natl. Acad. Sci. U.S.A.*, 2002, **99**, pp. 16742-16747.
30 Gessel MM, Bernstein S, Kemper M, Teplow DB & Bowers MT, *ACS Chem Neurosci*, 2012, **3**, pp. 909-918.
31 Berhanu WM, Hansman UHE, *PloS ONE,* 2012, **7**, e41479

32 Tycko R & Wickner RB, *Acc. Chem. Res.*, 2013, **46**, pp. 1487-1496.
33 Lazo ND, Grant MA, Condron MC, Rigby AC & Teplow DB, *Protein Sci.*, 2005, **14**, pp. 1581-1596.
34 Cruz L, Urbanc B, Borreguero JM, Lazo ND, Teplow DB & Stanley HE, *Proc. Natl. Acad. Sci. U.S.A.*, 2005, **102**, pp. 18258-18263.
35 Cruz L, Rao JS, Teplow DB & Urbanc B, *J Phys Chem B*, 2012, **116**, pp. 6311-6325.
36 Fawzi NL, Phillips AH, Ruscio JZ, Douclef M, Wemmer DE & Head-Gordon T, *J. Am. Chem. Soc.*, 2008, **130**, pp. 6145-6158.
37 Murray MM, Krone MG, Bernstein SL, Baumketner A, Condron MM, Lazo ND, Teplow DB, Wyttenbach T, Shea J & Bowers MT, *J Phys Chem B*, 2009, **113**, pp. 6041-6046.
38 Borreguero JM, Urbanc B, Lazo ND, Buldyrev SV, Teplow DB & Stanley HE, *Proc. Natl. Acad. Sci. U.S.A.*, 2005, **102**, pp. 6015-6020.
39 Fawzi NL, Phillips AH, Ruscio JZ, Doucleff M, Wemmer DE & Head-Gordon T, *J. Am. Chem. Soc.*, 2008, **130**, pp. 6145-6158.
40 Baumketner A, Bernstein SL, Wyttenbach T, Lazo ND, Teplow DB, Bowers MT & Shea J, *Protein Sci.*, 2006, **15**, pp. 1239-1247.
41 Tarus B, Straub JE & Thirumalai D, *J. Mol. Biol.*, 2008, **379**, pp. 815-829.
42 Chen W, Mousseau N & Derreumaux P, *J Chem Phys*, 2006, **125**, p. 084911.
43 Jorgensen WL, Maxwell DS & Tirado-Rives J, *J. Am. Chem. Soc.*, 1996, **118**, pp. 11225-11236.
44 Kaminski G & Jorgensen WL, *Journal of Physical Chemistry*, 1996, **100**, pp. 18010-18013.
45 Jorgensen W, Chandrasekhar J, Madura J, Impey R & Klein M, *Journal of Chemical Physics*, 1983, **79**, pp. 926-935.
46 Berendsen HJC, Van der spoel D & Vandrunen R, *Computer Physics Communications*, 1995, **91**, pp. 43-56.
47 Van der Spoel D, Lindahl E, Hess B, Groenhof G, Mark AE & Berendsen HJC, *Journal of Computational Chemistry*, 2005, **26**, pp. 1701-1718.
48 Hess B, Kutzner C, van der Spoel D & Lindahl E, *Journal of Chemical Theory and Computation*, 2008, **4**, pp. 435-447.
49 Pronk S, Páll S, Schulz R, Larsson P, Bjelkmar P, Apostolov R, Shirts MR, Smith JC, Kasson PM, van der Spoel D, Hess B & Lindahl E, *Bioinformatics*, 2013, **29**, pp. 845-854.
50 Nguyen PH, Li MS, Derreumaux P. *Phys. Chem. Chem. Phys*, 2011, **13, 20**, pp. 9778-9788.
51 Lindorff-Larsen K, Maragakis P, Piana S, Eastwood MP, Dror RO, Shaw DE. *PLOS ONE*, 2012, **7**, **2**, e32131.
52 Patriksson A & Van der Spoel D, *Phys. Chem. Chem. Phys.,* 2008 **10**, pp. 2073-2077
53 Nose S, *Progress of Theoretical Physics*, 1991, pp. 1-46.
54 Parrinello M & Rahman A, *J. Appl. Phys.*, 1981, **52, 12**, pp. 7182-7190.
55 Nosé S & Klein ML, *Molecular Physics*, 1983, **50, 5**, pp. 1055-1076.
56 Smith MD & Cruz L, *J. Phys. Chem. B*, 2013, **117**, pp. 6614-6624.
57 Smith MD & Cruz L, *J. Phys. Chem B.*, 2013, **117**, pp. 14907-14915
58 Rao JS & Cruz L, *J Phys Chem B*, 2013, **117**, pp. 3707-3719.
59 Frishman D & Argos P, *Proteins: Structure, Function, and Genetics*, 1995, **23**, pp. 566-579.
60 Heinig M & Frishman D, *Nucleic Acids Res.*, 2004, **32**, pp. W500-2.

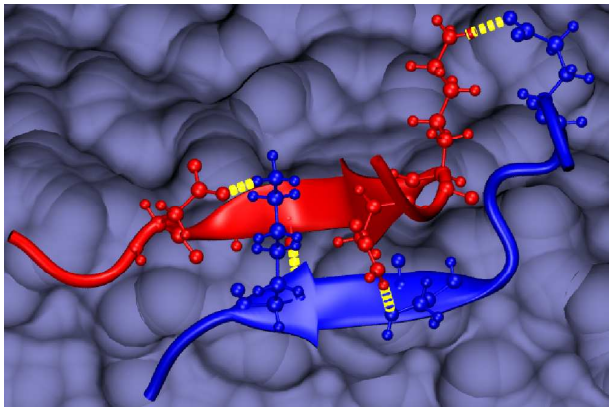

Computation examination of the spontaneous dimerization of $A\beta_{21-30}$ and stability measures of the resulting parallel and anti-parallel aligned dimers.